Grid-forming VSC control in four-wire systems with unbalanced nonlinear loads

Lliuyacca, Ruben; Mauricioa, Juan M. ; Gomez-Exposito, Antonio; Savaghebi, Mehdi; Guerrero, Josep M.

Published in:
Electric Power Systems Research

DOI (link to publication from Publisher):
10.1016/j.epsr.2017.07.010

Publication date:
2017

Document Version
Early version, also known as pre-print

Grid-Forming VSC control in Four-Wire Systems with Unbalanced Nonlinear Loads

Ruben Lliuyacc[a], Juan M. Mauricio[a], Antonio Gomez-Exposito[a], Mehdi Savaghebi[b], Josep M. Guerrero[b]

[a]*Department of Electrical Engineering, University of Seville, Seville, Spain*
[b]*Department of Energy Technology, Aalborg University, Aalborg East DK-9220, Denmark*

Abstract

A grid-forming voltage source converter (VSC) is responsible to hold voltage and frequency in autonomous operation of isolated systems. In the presence of unbalanced loads, a fourth leg is added to provide current path for neutral currents. In this paper, a novel control scheme for a four-leg VSC feeding unbalanced linear and nonlinear loads is proposed. The control is based on two control blocks. A main control commands the switching sequence to the three-phase VSC ensuring balanced three-phase voltage at the output; and an independent control to the fourth leg drives neutral currents that might appear. The proposed control is noninvasive in the sense that both control blocks are independently implemented, avoiding the use of complex modulation techniques such as 3D-SVPWM. Moreover, the main control is deployed in *dqo* reference frame, which guarantees zero steady-state error, fast transient response during system disturbances and mitigation of harmonics when nonlinear loads are present. Simulations and experimental results are presented to verify the performance of the proposed control strategy.

Keywords: VSC, four-leg, unbalanced loads, nonlinear, neutral phase, isolated.

1. Introduction

Isolated microgrids can be defined as a cluster of distributed generation, energy storage devices and loads connected through a relatively small grid, usually at medium or low

Email addresses: rlliuyacc@us.es (Ruben Lliuyacc), j.m.mauricio@ieee.org (Juan M. Mauricio), age@us.es (Antonio Gomez-Exposito), mes@et.aau.dk (Mehdi Savaghebi), joz@et.aau.dk (Josep M. Guerrero)

voltage levels. Storage devices and distributed generation, such as photovoltaic arrays, fuel cells and wind turbines are customarily connected to the microgrid through power electronic interfaces that include DC/AC converters [1, 2]. These converters can be operated in two modes: grid-feeding mode and grid-forming mode. In grid-feeding mode, the converter supplies a given active and reactive power set points. Active power set point is subject to power availability from the primary resource (wind, sun, etc.), while reactive power is predefined either locally or through a central control [3]. In grid-forming mode, the converter seeks to control a predefined frequency and voltage, for which it is usually connected to a storage system. Nowadays, the preferred converter topology, at least for the grid-forming role, is the IGBT-based Voltage Source Converter (VSC) type [4, 5].

Fig.1 shows a common configuration in real microgrid applications [6, 7], where there is a VSC which is responsible to hold voltage and frequency during isolated operation, substituting the main grid functions. Distributed generation (DG) represents the set of grid-feeding generation (i.e. PV, combined heat and power, wind, biomass) that only injects active and reactive power without taking any responsibility in improving the power quality of the grid (unbalances, stability, harmonics, flickers, etc.). These DGs can be seen as intermittent balanced and unbalanced negative loads as they can include single-phase PV generation. The connected loads can include linear and nonlinear type as well as three-phase and single-phase loads (i.e. electric vehicles). In this context, significant unbalances and harmonics can be found and must be duly considered by the grid-forming VSC to hold frequency and voltage at the point of interconnection (POI), regardless the type of load connected, and the disturbances caused by DGs during an isolated operation.

The first approaches to overcome unbalances were based on reactive power compensators (variants of Steinmetz circuit). Those approaches minimize or, under certain circumstances, eliminate unbalances by means of additional costly equipment such as active filters [8, 9], dynamic voltage restorers [10] or STATCOMs [11]. Other schemes deal with unbalances by trying to firmly hold a three-phase balanced voltage everywhere, regardless the type of loads. However, some of these methods are limited to unbalances with only negative-sequence component, neglecting the possible presence of a zero-sequence component circulating through

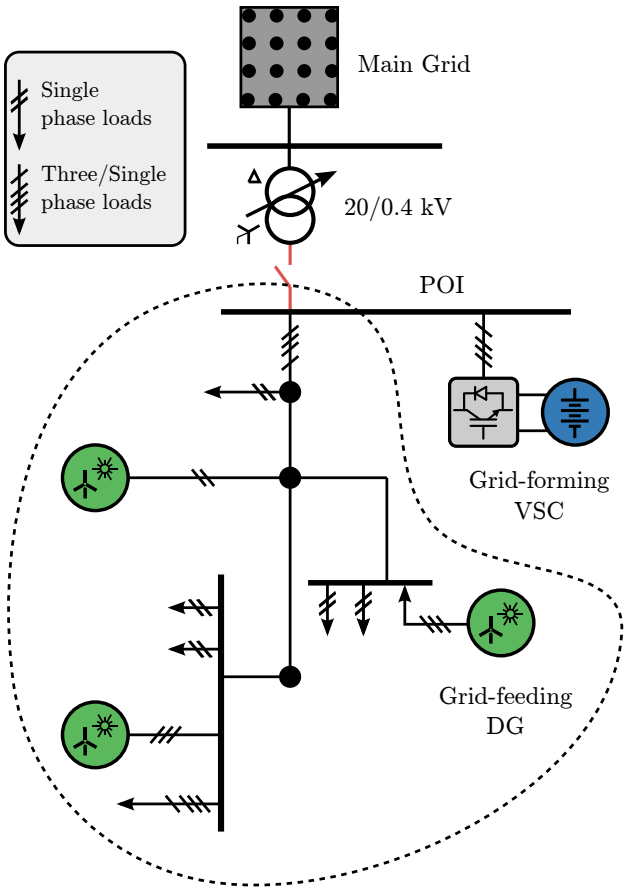

Figure 1: Common microgrid topology with one grid-forming VSC responsible to hold frequency and voltage during isolated operation.

a neutral phase [12–14].

In the most general unbalanced case, the neutral phase must be taken into account, for which two different topologies have been mainly proposed. The first is a split DC link, where the neutral phase is connected to the middle point of the DC link through an inductor filter. This alternative has proved to be unstable in case of large unbalances, unless huge capacitors are used to achieve equal voltage sharing between the split capacitors. Thus, this topology may be infeasible for real implementation on DC-AC voltage converters[15]. The second topology consists of adding a fourth leg to the conventional three-leg VSC, commonly known as four-leg VSC (4LVSC), so that the neutral current can be directly and independently driven through this additional leg. Available control techniques for this

configuration can be classified in three groups, depending on the reference frame they use: *abc* frame, $\alpha\beta o$ frame, and *dqo* frame. A survey of advantages and disadvantages arising from the use of each reference frame is presented in [16]. Although there is no absolute consensus of what reference frame is the best for VSC control applications, the *dqo* reference frame excels in the following points: 1) simple control structure, 2) zero error in steady-state and fast transient responses, and 3) fixed switching frequency. Therefore, it is chosen as a reference frame to develop the main control in this paper.

All the techniques that exploit *dqo* reference frame use 3D-SVPWM (Three-dimensional Space Vector Pulse Width Modulation) as an interface between the control's output and the switching sequence for the 4LVSC [17–24]. Such a modulation method, however, exhibits high computational cost, and it is difficult to implement even when using a fast DSP control platform [25, 26]. Moreover, those techniques also suffer from any of the following shortcomings: communication infrastructure required [19], control capability limited to only linear loads [17] or resistive loads [18], which can be extended to inductive and capacitive components with certain modifications [18, 22], the coupling between voltage/current inner control loops is neglected [22].

The control proposed in this paper overcomes the aforementioned issues by using simple PWM (Pulse Width Modulation) for both the three-phase VSC (main control) and the fourth leg. Furthermore, taking advantage of the *dqo*-frame features described above, the main control loop is devoted to deal with both linear and nonlinear loads, whereas the independent control of the fourth leg uses a PR controller to drive neutral currents. In brief, the main features and contributions of this work can be summarized in the following points:

- Use of simple PWM for both the main control and the fourth leg control of the VSC.
- Truly independent control of the fourth leg, allowing a noninvasive implementation.
- Main control deployed in *dqo* reference frame, hence achieving zero steady-state error and fast transient response during system disturbances.
- Valid for all type of loads.

- No communication infrastructure required.

The rest of the paper is outlined as follows: Section II introduces the VSC control in *dqo* reference frame by using symmetrical decomposition. Section III presents a novel 4LVSC control consisting of a main control for the three-phase VSC and an independent control applied to the fourth leg. The results and discussion are presented in Section IV. Finally, the conclusions are drawn in Section V.

2. VSC Control Based on Symmetrical Components

In an isolated microgrid, VSCs must set the reference for voltage and frequency. This makes it to work as a voltage source from the point of view of the rest of the microgrid. For this purpose, a capacitor bank is attached between the inductor and the POI where the voltage has to be controlled, as shown in Fig. 2a.

A cascaded control strategy where one controller takes care of the capacitor voltage, while generating references to another controller in charge of the inductor currents, is the most common approach [5]. In Fig. 2b, these controllers are highlighted as *Voltage Control Loop* and *Current Control Loop*, respectively. The controllers could be formulated in *dq* frame where the typical coupling between d and q components can be eliminated using the decoupling terms indicated in the same figure. Using proportional-integral controllers (PI), good transient performance and almost null steady-state error can be achieved.

The control of an isolated VSC in *dq* reference frame, based on symmetrical decomposition, is shown in Fig. 2a[27, 28]. Three-phase voltage and current measurements are transformed into *dq* reference frame for each symmetrical component (positive, negative and homopolar). Then, a control based on two inner control loops is deployed for each of the symmetrical component control blocks. The aims of this control is to set a frequency and a three phase voltage at the POI. For that, $v^{\star}_{pd}$ reference value sets the output voltage while the others $(v^{\star}_{pq}, v^{\star}_{nd}, v^{\star}_{nq}, v^{\star}_{hd}, v^{\star}_{hq})$ are set to zero to ensure a balanced output voltage. The outputs of each symmetrical component control blocks are transformed to *abc* reference frame and then added together resulting in the duty signal that goes to the simple PWM

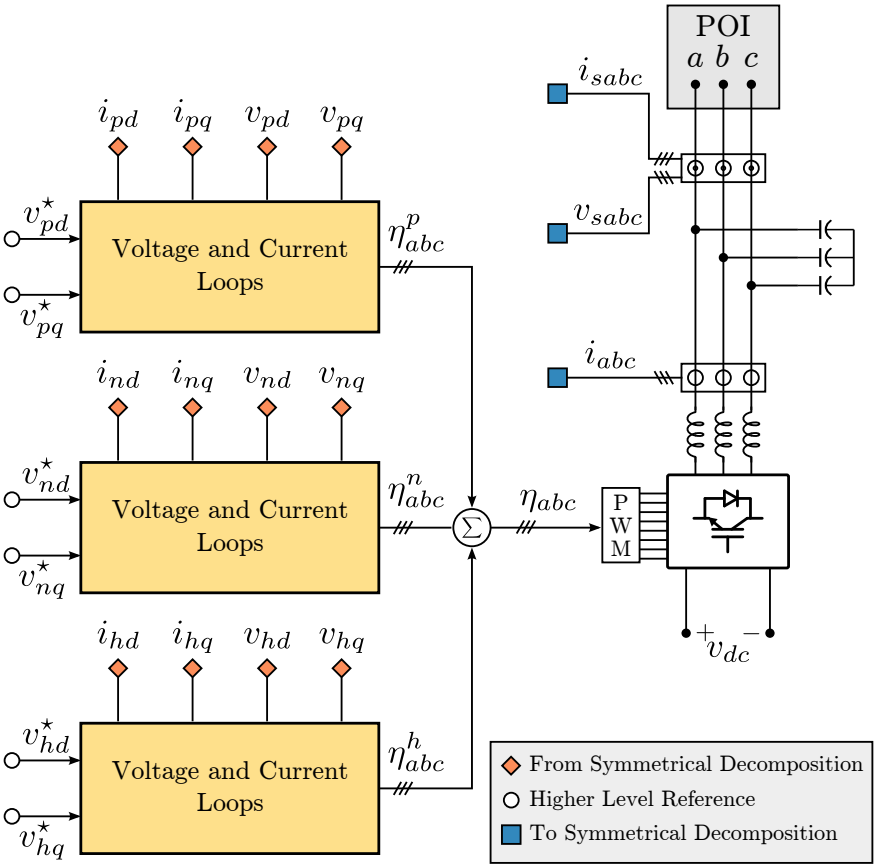

(a)

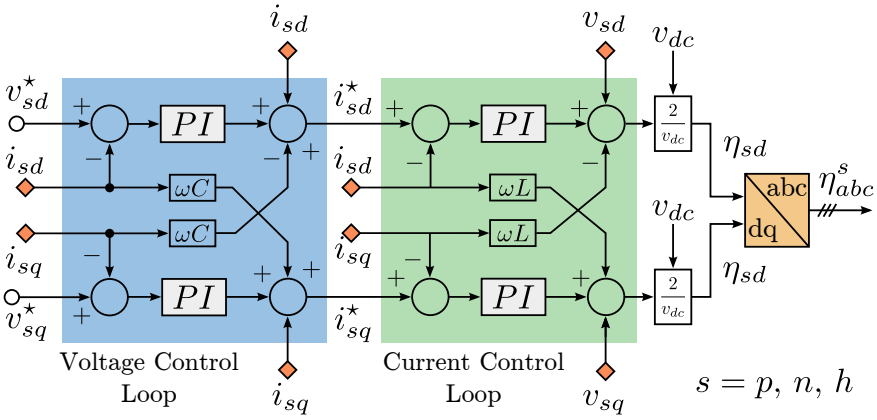

(b)

Figure 2: (a) VSC control based on symmetrical components. (b) Voltage and current control loops.

which commands the switching sequence for the VSC. However, this control neither works with nonlinear loads nor includes the control of the fourth leg, and therefore cannot cope with unbalanced loads with neutral current component.

3. Proposed Control Strategy for the 4LVSC

3.1. Main Control for Linear and Nonlinear loads

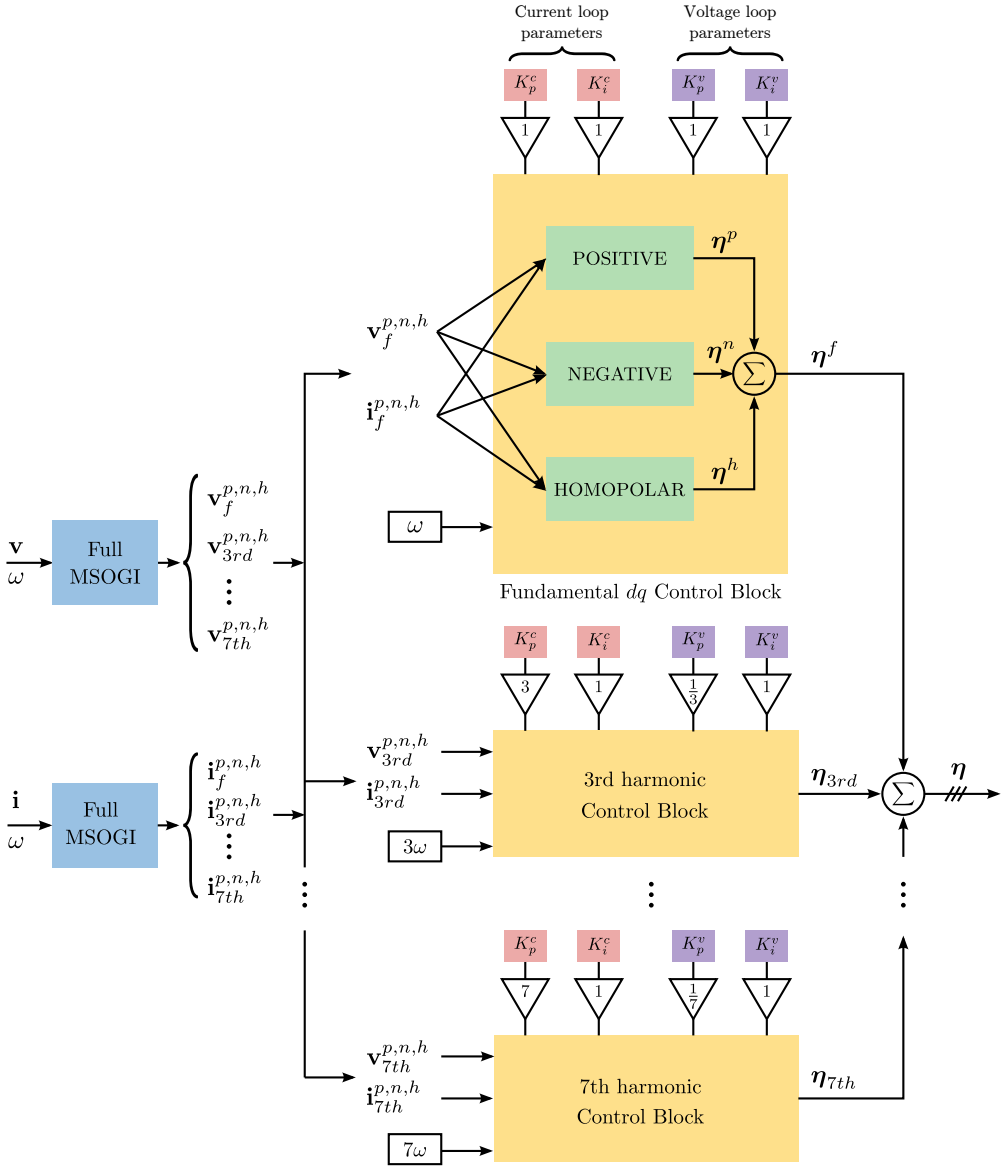

Figure 3: Proposed main control for non linear loads in *dq* reference frame.

The main control described in section II is only valid for linear loads (balanced or unbalanced with only negative sequence component). Therefore, under the presence of nonlinear loads the aforementioned control is not able to hold a three-phase sinusoidal voltage at the POI. Nonlinear loads are mostly handled by using resonant controllers in $\alpha\beta o$ reference frame [29, 30]. To the authors knowledge, no work has dealt with nonlinearity in the *dqo* reference frame, mainly because the generalization of symmetrical decomposition to non-sinusoidal three-phase signals has not been satisfactorily addressed [31, 32]. However, the attributes of *dqo* reference frame are well worth exploring in order to deploy a control for nonlinear loads in that domain, like the one presented in this section. Fig. 3 shows a block diagram of the proposed control where the idea is to consider separate control blocks for fundamental and harmonic signals in *dqo* frame. For this purpose, voltage and current measurements are split into positive, negative and homopolar sequences for the fundamental, 3rd, 5th and 7th harmonics (as main harmonic components), using an extended version of the multiple second-order generalized integrator (MSOGI) proposed in [33]. The MSOGI extracts only the positive and negative sequences of the fundamental and main harmonics ($\mathbf{x}_f^{p,n}, \mathbf{x}_{3rd}^{p,n}, .., \mathbf{x}_{7th}^{p,n}$) of a three-phase signal $\mathbf{x}$. The proposed extended version (Full-MSOGI) resorts to an additional algorithm aimed at extracting the homopolar sequence, as shown in Fig.4. The added block is based on the same principle of extraction as MSOGI, that is, a cross-feedback structure consisting of multiple SOGI quadrature signal generators (SOGI-QSGs), tuned at different frequencies in proportion to the angular frequency set point ω. Tuning criteria (value of k) for the SOGI-QSG's are based on [33]. The resulting homopolar outputs ($\mathbf{x}_f^h, \mathbf{x}_{3rd}^h, .., \mathbf{x}_{7th}^h$) have to appear as a three-phase signal, so that a *dqo* transformation can be performed afterwards (for the symmetrical component control blocks), allowing a spatial rotation of 120° and 240° to be applied to the single-phase signals $x_f, x_{3rd}, x_{5th}, x_{7th}$. For this purpose, the $\alpha\beta$ transformation matrix (TM) is used,

$$\mathbf{x}_{ith}^h = [TM][x_{ith}; x'_{ith}] \quad TM = \begin{bmatrix} 0 & -\sqrt{3}/2 & \sqrt{3}/2 \\ 1 & -1/2 & -1/2 \end{bmatrix}^T \tag{1}$$

where ith represents the harmonic's order.

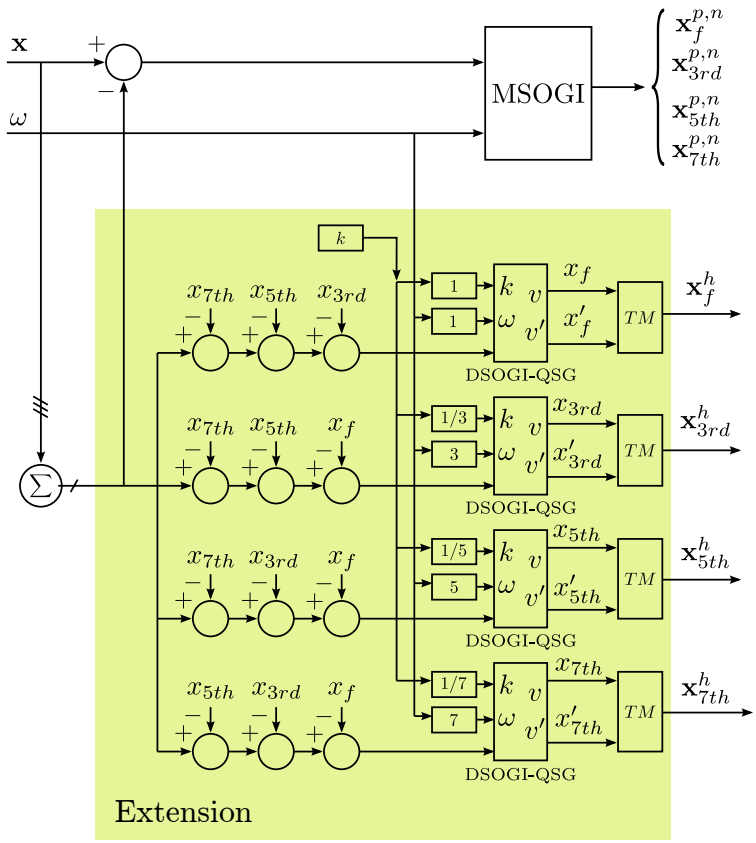

Figure 4: Full-MSOGI: MSOGI [33] plus an extension (shaded area) to include homopolar sequence extraction of signal $\mathbf{x}$.

After Full-MSOGI extraction, the signals ($\mathbf{x}_f^{p,n,h}$, $\mathbf{x}_{3rd}^{p,n,h}$, ..., $\mathbf{x}_{7th}^{p,n,h}$) are sent to the corresponding fundamental and harmonic control blocks (see Fig. 3), where the symmetrical component's principle is separately applied to yield a *dqo* control based on the voltage/current control loops shown in Fig. 2b. The bandwidth of the current regulator for the fundamental control block (k_p^c) is adapted to the 3rd, 5th and 7th harmonics control blocks by multiplying its value by a coefficient that determines the order of the harmonic (1, 3, 5, ..). Analogously, the proportional gains in each voltage regulator (k_p^v) is divided by the corresponding harmonic order to keep the product constant, which guarantees the same bandwidth for all control blocks. Same values for the integral gains (k_i^c, k_i^v) for both current and voltage control loops are set for all control blocks. Finally, duty cycles of fundamental and harmonics control blocks ($\boldsymbol{\eta}_f, \boldsymbol{\eta}_{3rd}, .., \boldsymbol{\eta}_{7th}$) are added to get $\boldsymbol{\eta}$, which goes to the PWM associated with

the three-phase VSC.

3.2. Independent Fourth Leg Control

As mentioned before, among the alternatives to introduce a neutral wire in a VSC, adding a fourth leg is the more feasible solution to handle unbalances, and even nonlinear loads [16]. The techniques developed in the *dqo* reference frame link the control of the fourth leg with the main control of the VSC, by using 3D-SVPWM. Besides working only for linear loads, this involves complex calculation and high computational cost.

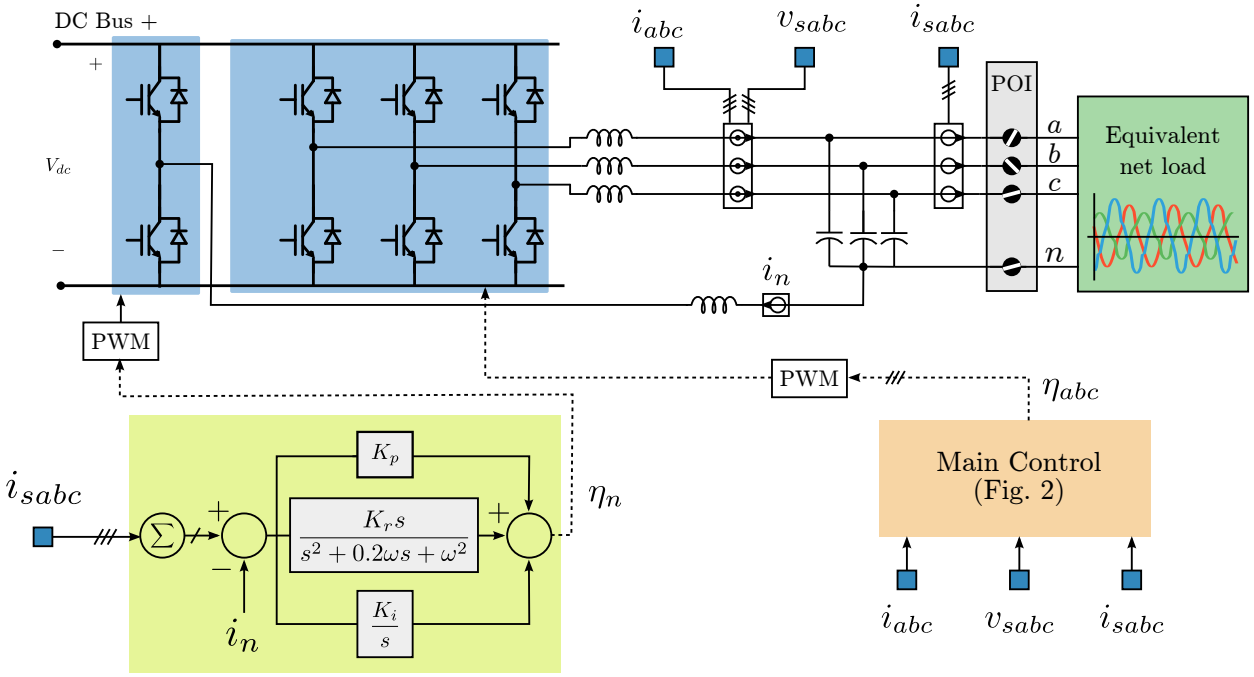

Figure 5: Proposed grid-forming 4LVSC control based on two control blocks: a main control deployed in *dqo* frame and an independent control using a resonant controller.

Fig. 5 shows the control scheme for the 4LVSC where a neutral phase is introduced. The main control, based on the inner current and outer voltage control loops, commands the switching sequence for the three-leg VSC. These control loops are developed in a *dq*0 reference frame for each (positive, negative, and homopolar) sequence and for each fundamental and harmonics control blocks, as shown in Fig. 3. The independent control (leftmost lower block in Fig. 5) is based on a Proportional-Integral Resonant (PIR) controller, which is only

responsible to give the switching sequence to the fourth leg. The transfer function of the PIR is given by:

$$G_s = K_p + \frac{K_r s}{s^2 + w_{cut} s + w_o^2} + \frac{K_i}{s} \tag{2}$$

where K_p is the proportional constant, K_r is the resonant constant for the frequency component w_o, w_{cut} is the cutoff frequency and K_i represents the integral part that attenuates DC components that might appear.

The idea of the independent control is to produce a voltage in the middle of the fourth leg so that the current entering this terminal equals the measured neutral current, in case a non-null neutral current is present. For that purpose, three-phase output current i_{abc} is measured, and the reference neutral current is computed based on the sum of phase currents. The error between the reference and the fourth leg's actual current i_n is the input for the PIR controller. PIR's output gives the duty signal to the single phase PWM in order to generate a voltage v_n that produces the desired current.

4. Results and Discussion

Fig. 5 shows the three-phase four-wire test system considered for simulation and experimental validation of the proposed control. The isolated system consists of a 4LVSC connected at the POI, which feeds a net load representing the set of grid-feeding DGs, the actual passive loads (possibly unbalanced and/or nonlinear) and the distribution system losses (as shown by the dashed area in Fig.1), all of them replaced hereafter by a single-port Thevenin equivalent for simulation and experimental purposes.The main parameters used are shown in Table 1.

4.1. Simulations results

The validation of the proposed control strategy is firstly done by means of simulations using the same parameters of the experimental setup. Simulations are performed using detailed models from SimPowerSystems^{TM} in MATLAB/Simulink^{TM}. The objective of the control is to hold a three-phase sinusoidal balanced voltage during unbalanced and nonlinear load

Table 1: System parameter for the study

Parameters	
Rated Power	2.2 kVA
Frequency	50 Hz
AC Voltage	400 V
DC Voltage	800 V
Switching Freq.	10 kHz
LC Filter Inductance	1.8 mH
LC Filter Capacitance	35 uF
k	1.4142
k_p^c	9.0
k_i^c	500
k_p^v	0.035
K_p	0.01
K_r	10.0
K_i	0.001
w_{cut}	2 Hz

conditions while driving the neutral current that might appear. To test the proposed control performance, three load conditions are considered, namely: balanced load, unbalanced load, and extremely unbalanced load (single-phase).

Fig. 6 shows the results obtained. At $t = 0$, a balanced linear load of 0.65 kW is connected ($R_{a,b,c} = 240\Omega$). As expected, the output voltage and current are balanced and the neutral current is zero. Then at $t = 0.1\,s$, the balanced load is increased to 2 kW ($R_{a,b,c} = 80\Omega$). Still, there are no unbalances, hence the current at the neutral phase is zero as shown in the figure. Moreover, although the independent control for the fourth leg is actually operating at this point (with $i_{ref} = 0$), it does not disturb the performance of the three-phase VSC's main

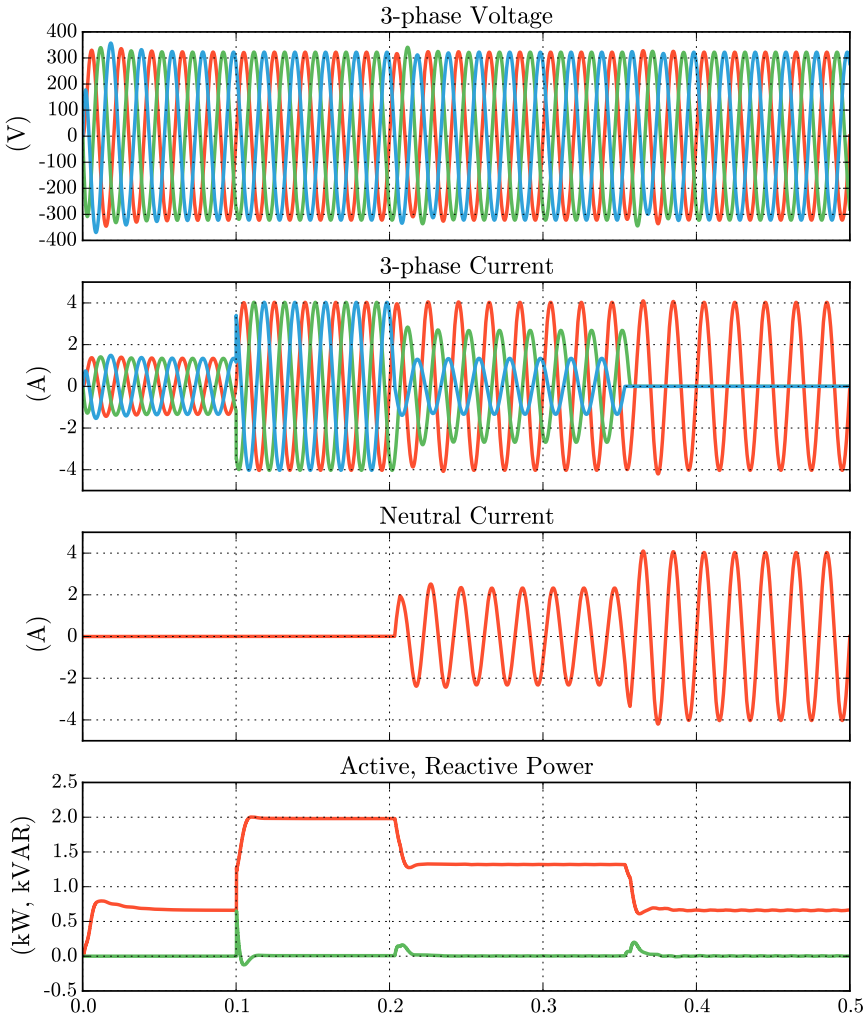

Figure 6: Results obtained in simulations by applying the proposed control.

control. At $t = 0.3\,s$, unbalances are introduced by changing differently the consumption of each phase ($R_a = 80\Omega$, $R_b = 120\Omega$, and $R_c = 240\Omega$). As a result, a neutral current starts to circulate and it is all driven by the proposed control to the fourth leg while VSC output voltage remains balanced and sinusoidal. Finally, at $t = 0.4\,s$ only a single-phase load remains connected between phase a and the neutral point ($R_a = 80\Omega$). Yet, even for such extreme unbalanced condition, the output voltage is kept balanced.

As the control of the fourth leg is independent from the main three-phase VSC control, keeping a three-phase balanced output voltage is a matter of the main control. Whenever there is a neutral current in the load, the proposed control acts independently deriving

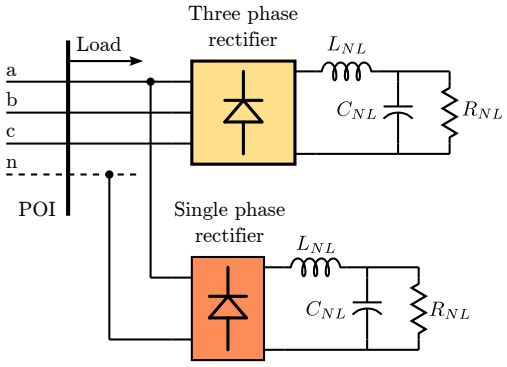

Figure 7: Test unbalanced nonlinear load.

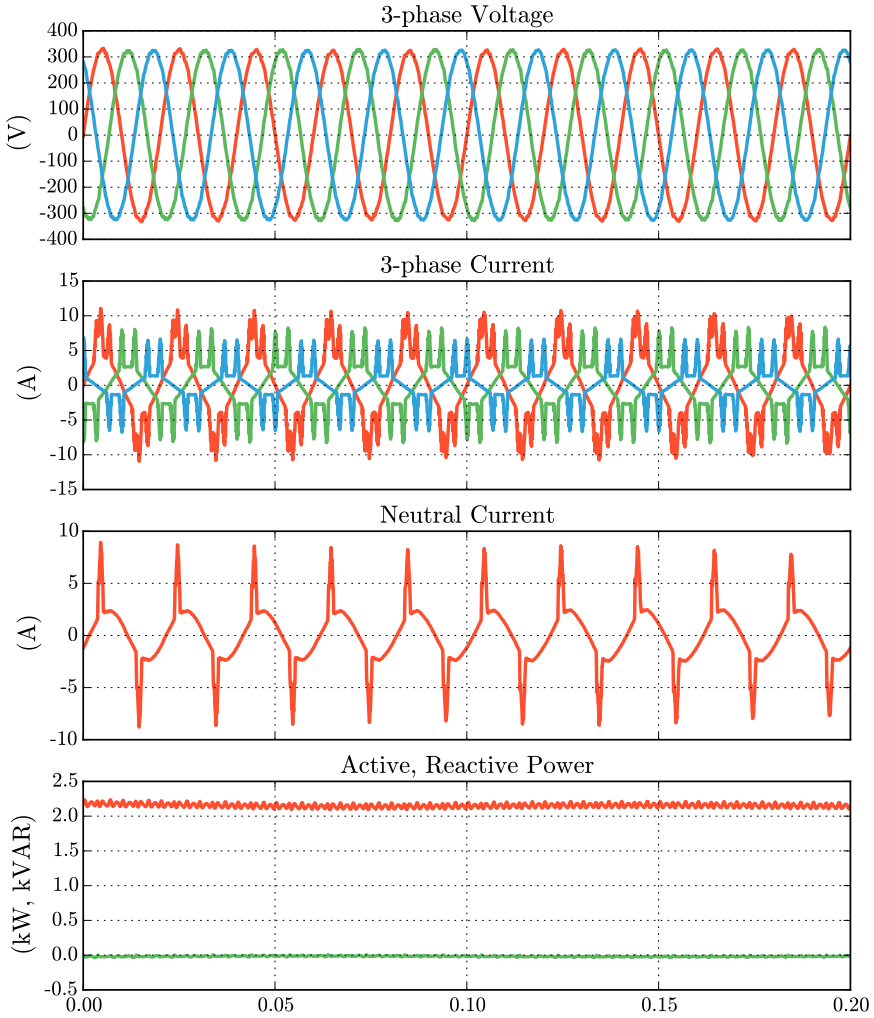

Figure 8: Versatility of the proposed control under nonlinear unbalanced loads with neutral current.

this current to the fourth leg. This shows the versatility of the proposed control to be implemented for both linear and nonlinear unbalanced loads. In the next simulation, an unbalanced nonlinear load is created by connecting a three-phase diode rectifier feeding passive linear components ($L_{NL} = 0.08mH$, $C_{NL} = 235uF$, and $R_{NL} = 500\Omega$) and a single-phase diode rectifier of the same features between phase a and n, both at POI, as shown in Fig. 7. The performance of the proposed control in these scenarios is shown in Fig. 8. As the 4LVSC is connected to a nonlinear load with homopolar component, a non-sinusoidal current flows through the neutral phase. The main control compensates the voltage harmonics and keeps the output voltage balanced, while the independent control derives the resulting current to the fourth leg.

4.2. Experimental results

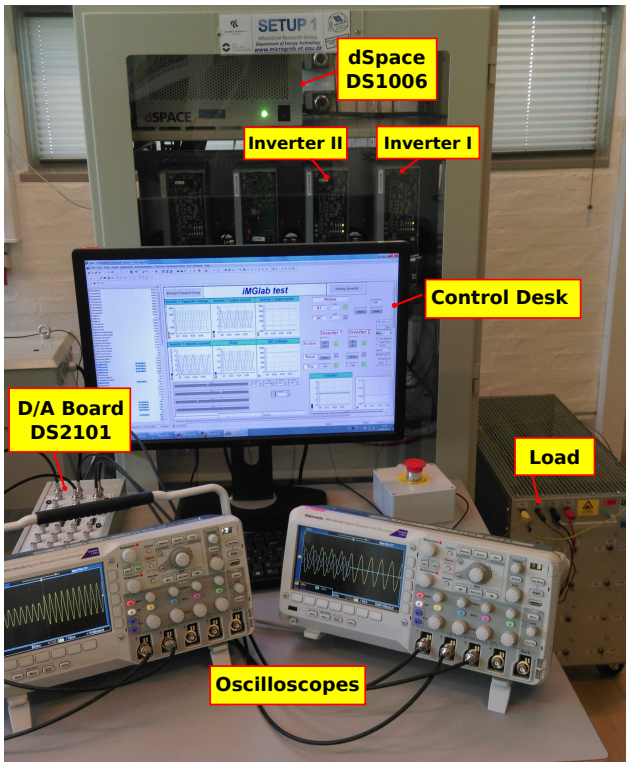

Figure 9: Experimental setup.

The system in Fig. 5 was tested experimentally. For this purpose, a laboratory prototype has been built using two three-leg Danfoss^{TM} 2.2 kW inverters, driven by a DSpace^{TM}

DS1006 platform. An Analog-to-Digital DS2004 board is used to digitalize the analog signals sensed via current and voltage transducers. A 16-bit high resolution Digital-to-Analog conversion board DS2102 is used to monitor the signals with oscilloscopes. A photo of the experimental setup is shown in Fig. 9. Inverter I works as a three phase VSC whereas Inverter II provides one leg (keeping the two others legs inoperative) to build the four wire system.

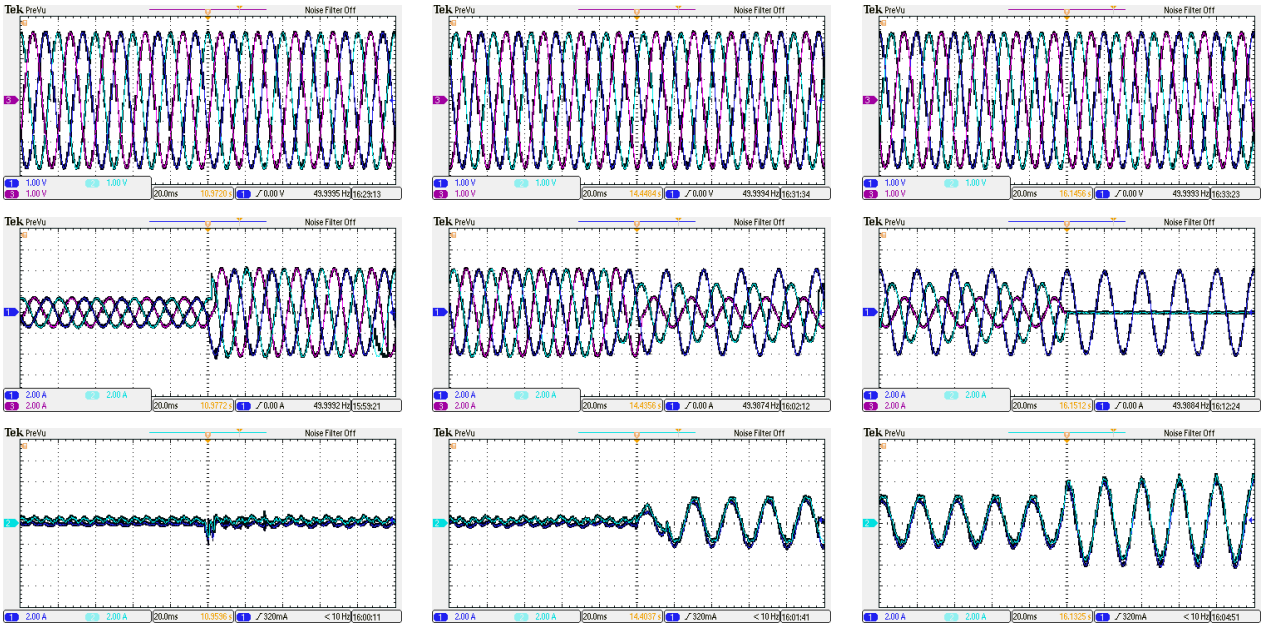

(a) (b) (c)

Vertical axis from top to bottom: Output voltage (100v/div), output current (2A/div), reference and measured neutral current (2A/div).

Figure 10: Oscilloscope's outputs during different load conditions: (a) Increased power of balanced load. (b) Unbalanced load is introduced. (c) Single-phase load only.

The system was tested under three load changes to verify the capability of the proposed control, much like in the simulated scenarios. First, the response upon a sudden increase of power was tested, for which an initial balanced load was increased from 0.66 kW to 2kW ($R_{a,b,c}$ from 240 to 80 Ω). As shown in Fig. 10 (a), the output voltage remains stable under this disturbance.

Second, an unbalanced load ($R_a = 80\Omega$, $R_b = 120\Omega$, and $R_c = 240\Omega$) is connected

while the voltage remains balanced as shown in Fig. 10 (b). The introduction of unbalances produces a neutral current in the system which is driven by the proposed independent control to the four leg, closing in this way the electrical circuit. The main control ensures that negative and homopolar sequences in the output voltage are mitigated, keeping it balanced.

Finally, to prove the robustness of the control, it is tested under extremely unbalanced conditions, which is a single-phase load connected between an individual phase and the neutral phase. Fig. 10 (c) shows the results where the output voltage remains balanced, and the output currents go entirely through the neutral phase to the fourth leg, matching the reference imposed to the independent control. The active and reactive output power for each load condition are pictured in Fig. 11, where each sub-figure (a), (b), and (c) corresponds to the load variations shown in Fig. 10. Since the loads are only resistive, the reactive power consumed is null in all the scenarios.

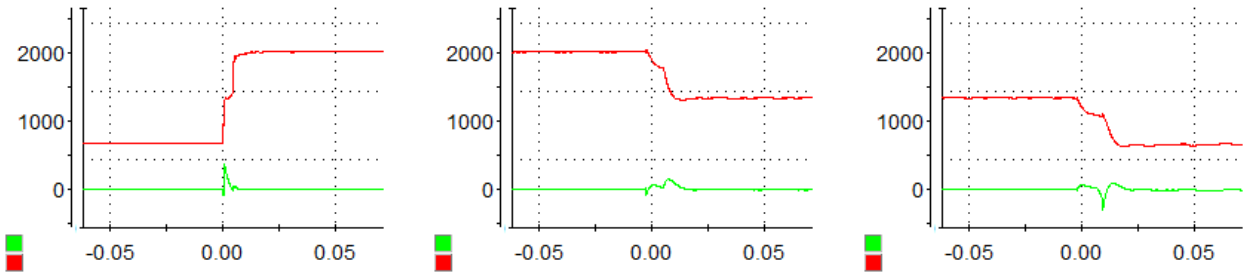

(a) (b) (c)

Figure 11: Three-phase active (red) and reactive (green) power during different load conditions.

Nonlinear loads are tested for two conditions: balanced and unbalanced. First, under a three-phase diode rectifier load ($L_{NL} = 0.08mH$, $C_{NL} = 235\mu F$, and $R_{NL} = 400\Omega$), the output phase voltage has a THD of just 1.5% while the current has a THD of 58%, the dominant current harmonics being the 5th and 7th as displayed in Fig. 12a. Second, the phase c of the previous diode rectifier load is unplugged in order to get triplen harmonics, thus an unbalanced nonlinear load. In this case, the output phase voltage has a THD of 1.9% while phase a and b currents have a THD of 92.5% with the dominant harmonics being the 3rd, 5th, 7th and 9th, as displayed in Fig. 12b. The performance of the main control in

the *dqo* reference frame proved to be good enough in compensating the harmonics present in the output voltage when dealing with nonlinear loads.

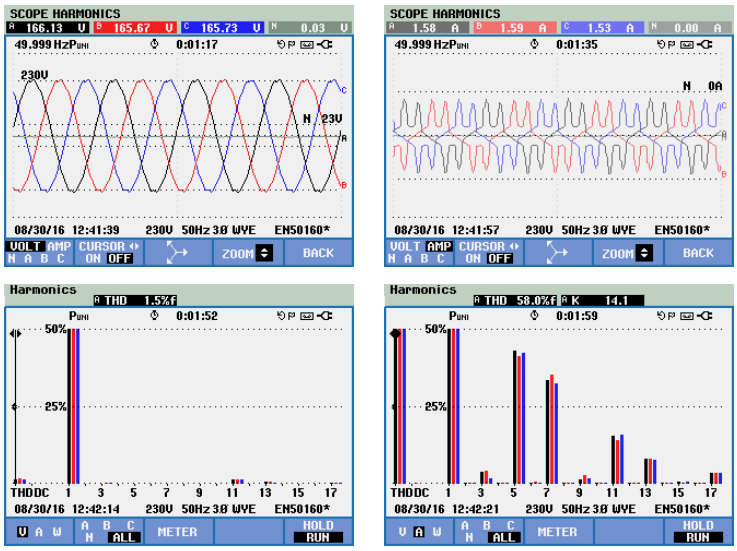

(a)

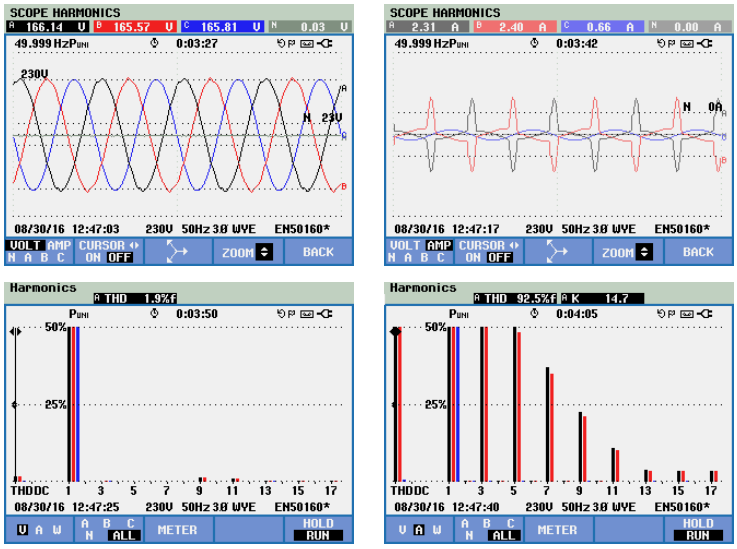

(b)

Figure 12: Three-phase Fluke power quality analyzer outputs at the POI under nonlinear load. (a) Balanced load. (b) Unbalanced load.

5. Conclusions

In this paper, a novel control for a four-leg VSC under unbalanced linear and nonlinear loads has been presented. The main control takes advantage of *dqo* reference frame attributes to deal with linear and nonlinear loads by redistributing the control into positive, negative and homopolar sequence for each fundamental and harmonic components. The fourth leg is controlled using a really independent PIR controller whose implementation does not require to modify the main control of the three-phase VSC. Moreover, the complexity of the control is reduced by using a simple PWM for the fourth leg, avoiding in this way complex modulation techniques such as 3DSVM. The performance of the proposed control has been proven in transient and steady state conditions by simulation and experimental tests.

Acknowledgements

This work was supported by the European Union through the ADVANTAGE Project under Grant 607774.

References

[1] J. M. Guerrero, M. Chandorkar, T.-L. Lee, P. C. Loh, Advanced control architectures for intelligent microgrids, part i: decentralized and hierarchical control, IEEE Transactions on Industrial Electronics 60 (4) (2013) 1254–1262.

[2] A. Bidram, A. Davoudi, Hierarchical structure of microgrids control system, IEEE Transactions on Smart Grid 3 (4) (2012) 1963–1976.

[3] J. Peas Lopes, C. Moreira, A. Madureira, Defining control strategies for microgrids islanded operation, Power Systems, IEEE Transactions on 21 (2) (2006) 916–924.

[4] T. Green, M. Prodanović, Control of inverter-based micro-grids, Electric Power Systems Research 77 (9) (2007) 1204–1213.

[5] J. Rocabert, A. Luna, F. Blaabjerg, P. Rodriguez, Control of power converters in ac microgrids, Power Electronics, IEEE Transactions on 27 (11) (2012) 4734–4749.

[6] N. Lidula, A. Rajapakse, Microgrids research: A review of experimental microgrids and test systems, Renewable and Sustainable Energy Reviews 15 (1) (2011) 186–202.

[7] T. S. Ustun, C. Ozansoy, A. Zayegh, Recent developments in microgrids and example cases around the worlda review, Renewable and Sustainable Energy Reviews 15 (8) (2011) 4030–4041.

[8] P. Lohia, M. K. Mishra, K. Karthikeyan, K. Vasudevan, A minimally switched control algorithm forthree-phase four-leg vsi topology tocompensate unbalanced and nonlinear load, IEEE Transactions on Power Electronics 23 (4) (2008) 1935–1944.

[9] A. Garcia-Cerrada, O. Pinzon-Ardila, V. Feliu-Batlle, P. Roncero-Sánchez, P. García-González, Application of a repetitive controller for a three-phase active power filter, IEEE Transactions on Power Electronics 22 (1) (2007) 237–246.

[10] G. Chen, M. Zhu, X. Cai, Medium-voltage level dynamic voltage restorer compensation strategy by positive and negative sequence extractions in multiple reference frames, IET Power Electronics 7 (7) (2014) 1747–1758.

[11] T.-L. Lee, S.-H. Hu, Y.-H. Chan, D-statcom with positive-sequence admittance and negative-sequence conductance to mitigate voltage fluctuations in high-level penetration of distributed-generation systems, IEEE Transactions on Industrial Electronics 60 (4) (2013) 1417–1428.

[12] B. Singh, J. Solanki, Load compensation for diesel generator-based isolated generation system employing dstatcom, IEEE Transactions on Industry Applications 47 (1) (2011) 238–244.

[13] S. R. Arya, R. Niwas, K. K. Bhalla, B. Singh, A. Chandra, K. Al-Haddad, Power quality improvement in isolated distributed power generating system using dstatcom, IEEE Transactions on Industry Applications 51 (6) (2015) 4766–4774.

[14] M. Singh, L. A. Lopes, N. A. Ninad, Grid forming battery energy storage system (bess) for a highly unbalanced hybrid mini-grid, Electric Power Systems Research 127 (2015) 126–133.

[15] Q.-C. Zhong, L. Hobson, M. G. Jayne, Classical control of the neutral point in 4-wire 3-phase dc-ac converters, Electrical Power Quality and Utilisation. Journal 11 (2) (2005) 73–81.

[16] M. R. Miveh, M. F. Rahmat, A. A. Ghadimi, M. W. Mustafa, Control techniques for three-phase four-leg voltage source inverters in autonomous microgrids: A review, Renewable and Sustainable Energy Reviews 54 (2016) 1592–1610.

[17] I. Vechiu, O. Curea, H. Camblong, Transient operation of a four-leg inverter for autonomous applications with unbalanced load, Power Electronics, IEEE Transactions on 25 (2) (2010) 399–407.

[18] R. Cárdenas, R. Peña, P. Wheeler, J. Clare, C. Juri, Control of a matrix converter for the operation of autonomous systems, Renewable Energy 43 (2012) 343–353.

[19] W. Sinsukthavorn, E. Ortjohann, A. Mohd, N. Hamsic, D. Morton, Control strategy for three-/four-wire-inverter-based distributed generation, Industrial Electronics, IEEE Transactions on 59 (10) (2012) 3890–3899.

[20] C. Liu, F. Wang, H. Bai, High performance controller design with pd feedback inner loop for three-phase four-leg inverter, in: Industrial Electronics and Applications, 2009. ICIEA 2009. 4th IEEE Conference on, IEEE, 2009, pp. 1057–1061.

[21] H. Bai, F. Wang, D. Wang, C. Liu, T. Wang, A pole assignment of state feedback based on system matrix for three-phase four-leg inverter of high speed pm generator driven by micro-turbine, in: Industrial Electronics and Applications, 2009. ICIEA 2009. 4th IEEE Conference on, IEEE, 2009, pp. 1361–1366.

[22] R. Nasiri, A. Radan, Adaptive pole-placement control of 4-leg voltage-source inverters for standalone photovoltaic systems, Renewable energy 36 (7) (2011) 2032–2042.

[23] N. A. Ninad, L. Lopes, Per-phase vector control strategy for a four-leg voltage source inverter operating with highly unbalanced loads in stand-alone hybrid systems, International Journal of Electrical Power & Energy Systems 55 (2014) 449–459.

[24] A. Mohd, E. Ortjohann, N. Hamsic, W. Sinsukthavorn, M. Lingemann, A. Schmelter, D. Morton, Control strategy and space vector modulation for three-leg four-wire voltage source inverters under unbalanced load conditions, IET power electronics 3 (3) (2010) 323–333.

[25] J. Rodriguez, M. Rivera, J. W. Kolar, P. W. Wheeler, A review of control and modulation methods for matrix converters, IEEE Transactions on Industrial Electronics 59 (1) (2012) 58–70.

[26] R. Cardenas, R. Pena, P. Wheeler, J. Clare, Experimental validation of a space vector modulation method for a 4-leg matrix converter, in: Power Electronics, Machines and Drives (PEMD 2010), 5th IET International Conference on, IET, 2010, pp. 1–6.

[27] I. Vechiu, H. Camblong, G. Tapia, B. Dakyo, O. Curea, Control of four leg inverter for hybrid power system applications with unbalanced load, Energy Convers Management 48 (7) (2007) 2119–2128.

[28] A. E. Leon, J. M. Mauricio, J. A. Solsona, A. Gomez-Exposito, Adaptive Control Strategy for VSC-Based Systems under Unbalanced Network Conditions, IEEE Transaction on Smart Grid 1 (3) (2010) 311–319.

[29] F. de Bosio, L. A. Ribeiro, F. D. Freijedo, M. Pastorelli, J. M. Guerrero, Effect of state feedback coupling and system delays on the transient performance of stand-alone vsi with lc output filter.

[30] M. Savaghebi, A. Jalilian, J. C. Vasquez, J. M. Guerrero, Secondary control for voltage quality enhancement in microgrids, Smart Grid, IEEE Transactions on 3 (4) (2012) 1893–1902.

[31] P. Tenti, J. Willems, P. Mattavelli, E. Tedeschi, Generalized symmetrical components for periodic non-sinusoidal three-phase signals, Electrical Power Quality and Utilisation Journal 13 (1) (2007) 9–15.

[32] L. L. H. Costa, P. J. A. Serni, F. P. Marafão, An analysis of generalized symmetrical components in non sinusoidal three phase systems, in: COBEP 2011-11th Brazilian Power Electronics Conference, 2011, pp. 502–507.

[33] P. Rodríguez, A. Luna, I. Candela, R. Mujal, R. Teodorescu, F. Blaabjerg, Multiresonant frequency-locked loop for grid synchronization of power converters under distorted grid conditions, IEEE Transactions on Industrial Electronics 58 (1) (2011) 127–138.